Switching Nonlinear Model Predictive Control of Collaborative Railway Vehicles in Catenary Grids

Gian Paolo Incremona, *Senior Member, IEEE*, Alessio La Bella, *Member, IEEE*,
and Patrizio Colaneri, *Fellow, IEEE*

Abstract—This paper contributes to the railway control field by proposing a novel approach capable of making trains collaborate, while also minimizing both traction energy and power line losses in catenary grids. The train dynamics is captured by a combination of four operating modes, so that the formulation of a switched control problem naturally applies. This model is interfaced with that of the catenary grid, consisting of the electrical substations and transmission lines over the track. Relying on these models, an eco-drive control system is proposed based on an original switching nonlinear model predictive control (SNMPC). Being collaborative-conceived, the new SNMPC is compared and evaluated against a non-collaborative version of the controller by means of simulation case studies relying on real world test data, a validated train model, and measured track topology. We obtain that the proposed SNMPC outperforms the non-collaborative counterpart both in terms of traction energy and energy losses on the train rheostats and over the electrical lines. Thus, we demonstrate that the proposed SNMPC for collaborative eco-drive, based on the energy exchange between trains, has a potential positive impact for railway systems in catenary grids.

Index Terms—Model predictive control, railway vehicles, power systems, switched systems.

I. INTRODUCTION

HIGHLY automated and even autonomous vehicles are revolutionizing the transportation mobility, and this evolutionary step is becoming a reality also in the railway sector. Indeed, trains are highly efficient means of transportation due to their limited environmental impact in terms of pollutant emissions. However, energy consumption is significantly influenced by the driving style and the scheduled timetable [1]. Hence, railway control methods have been widely studied by researchers, in order to generate the optimal energy-efficient driving strategy and mitigate its negative effects by reducing energy consumption, power losses and, as a consequence, operating costs. In this context, railway control can regard both driver advisory systems (DASs), to assist the human driver by suggesting the input handles, and automatic train operation (ATO) systems [2]. This paper focuses specifically on DASs for trains in catenary grids.

A. Overview on energy-efficient train control

Most of the research in the railway field deals with the design of optimal energy-efficient strategies aimed at generating the sequence of switching points for the optimal driving regime taking into account a trade-off between energy consumption and travel time. Specifically, among solution methods for optimization, the Pontryagin's minimum principle is the most relevant, showing that there exist four possible optimal modes of operation, i.e., acceleration, cruising, coasting and braking. Hence, the control problem becomes that of finding the optimal sequence of such modes depending on the track features, timetable and speed constraints [3]. Such approaches are commonly referred to as eco-drive control. This control paradigm has been widely exploited in the literature for conventional vehicles with the objective of reducing fuel consumption, and possibly pollutant emissions, by finding appropriate control sequences for gas and brake pedal (see e.g., [4] and the references therein).

Another line of research is instead devoted to the so-called regenerative braking, which is a valid solution to reduce energy consumption by recovering braking energy, that otherwise would be lost as heat into the environment, see [5]–[7] among many others. More specifically, whenever a regenerative braking occurs, the train behaves as a current generator by providing energy to the power distribution system. This generated energy can be used to supply other trains within the same substation or can be used for other loads such as lighting in stations. Such a technique is particularly effective in commuter trains and metro trains due to the fact that their journey is often characterized by frequent stops. Therefore, regenerative braking systems represent a valuable technology, and it is feasible both for alternate current (AC) powered trains and direct current (DC) powered ones. Specifically, its implementation finds a natural application for AC networks, but it is also very promising to reduce the electricity demand in very dense suburban DC powered networks.

More recently, the regenerative braking approach has given rise to a new concept, based on energy sharing by collaboration among trains. Specifically, the regenerative braking energy is supplied to the catenary grid and used to accelerate other trains connected to the same electrical substation instead of demanding energy from the substation itself. This energy share not only reduces the load on the substation, but also allows to reduce losses during the energy transfer from the substation to the trains. In the literature this paradigm is indicated as collaborative eco-drive, and several works rely on

the optimization of the train timetables, so as to synchronize the train acceleration and deceleration to be able to maximize the sharing of the available regenerated energy, [8]–[10].

B. Contributions with respect to the state of the art

The main goal of this paper is to propose a novel optimal-based collaborative eco-drive control for suburban trains with DAS, connected to the catenary grids.

Optimal control for railway systems has a relatively long history (see, e.g., [11]–[13]), and, among the control solutions, model predictive control (MPC) is a valid option due to its intrinsic capability to take into account state and input constraints [14]. For instance, in [15], a nonlinear MPC (NMPC) is applied for energy efficient operation of trains taking into account inclination and curvature of the track, resistances and speed limits.

Although the train dynamics is continuous in nature, practical implementation for DASs requires a quantization of the input handles to advice the driver, according to the four different operation modes of the train previously mentioned. Hence, because of the switching nature of the input handle, it is straightforward to formulate the train nonlinear dynamics as a switched system (see e.g., [16] for related stability arguments), so that a switching nonlinear MPC (SNMPC) needs to be applied [17]–[20]. In [21], for instance, a shrinking horizon SNMPC is applied to solve an eco-drive control problem for metro trains.

The idea of coordinated vehicles in railway systems via predictive controllers has been instead investigated, e.g., in [22], where a distributed cooperative MPC has been designed for energy-efficient trajectory planning in case of multiple high-speed trains. In [23], a hierarchical MPC has been introduced for the coordination of electrical traction substation energy flows at a higher level, and on-route trains energy consumption at a lower level. Recently, exploiting an interpretation of trains as Markov stochastic processes, a dissension based approach combined with a SNMPC has been proposed in [24].

However, in all the above-mentioned cases, no knowledge of the catenary grid model is taken into account in the optimization problem. This grid is instrumental for the energy exchange among trains, and its effect needs to be considered. Here, relying on the switched model of the trains, we propose a SNMPC based on the model of the catenary grid, taking into account line losses together with those due to the rheostats dissipation, thus enabling the collaboration among trains by coordinating their energy exchanges. To the best of authors' knowledge, this is the first time that a collaborative eco-drive control problem, properly exploiting the catenary grid, is proposed.

In our formulation, the switched nature of the model enables to select a reduced set of feasible sequences to solve the eco-drive control problem in a computationally efficient way. Moreover, in order to cope with possible stringent performance specifications, a move-blocking input parametrization can be adopted to decrease the number of optimization variables, further reducing the computational complexity. Finally, in collaboration with the company Alstom rail transport, we present promising results obtained relying on real data of metro trains, assessing the proposed approach in comparison with a non collaborative eco-drive strategy.

C. Outline

The paper is organized as follows. In Section II the dynamic and electrical models of the trains together with the catenary grid model are introduced, and the eco-drive control problem is presented. In Section III the switched model of the train is discussed in detail and the proposed collaborative eco-drive control approach is designed relying on a SNMPC strategy. In Section IV an extensive simulation campaign based on real data in a realistic simulation environment is illustrated and discussed by shedding light on the advantages and practical feasibility of the proposal. Some conclusions are gathered in Section V, while the real data adopted for the simulations are given in Appendix A.

Notation: The notation used in the paper is mostly standard. Let $\mathbb{N}_0$ denote the set of natural numbers including zero, while $\mathbb{R}$ be the set of real numbers. Let X be a matrix, X' is its transpose, and $[X]_{i,j}$ is its element at row i and column j. The matrix $\mathbf{0}_{n,m}$ indicates a null matrix with n rows and m columns. Given a set $\mathcal{B}$, its cardinality is denoted as $|\mathcal{B}|$. Let $x \in \mathbb{R}$ be a signal, the function $\text{step}(x)$ is defined such that $\text{step}(x) = 1$ if $x > 0$, and $\text{step}(x) = 0$ if $x \leq 0$. The "and" logic operator is indicated with the symbol $\wedge$. Finally, for a given variable x, then $\overline{x}$ and $\underline{x}$ correspond to its upper and lower bounds, respectively.

II. MODELLING AND PROBLEM STATEMENT

The considered train and catenary grid models are hereafter introduced, and the eco-drive control problem is formulated.

A. Train model

Dynamic model: Consider the train body of constant mass M moving on a track having curvature radius $r(s) \in \mathbb{R}$ and slope $\alpha(s) \in \mathbb{R}$, with s being the longitudinal displacement, as shown in Fig. 1.
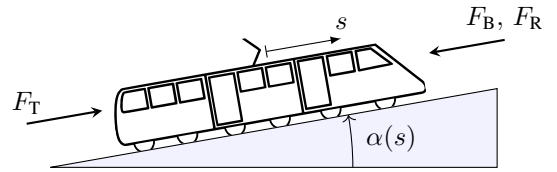

Fig. 1: Schematic force model of a train.

Letting T be the sampling time and $k \in \mathbb{N}_0$, the governing discrete-time model of motion is given by

$$\begin{cases} s_{k+1} &= s_k + T v_k, \\ v_{k+1} &= v_k + T \left(\frac{F_{\text{T}}(v_k, u_k) - F_{\text{B}}(v_k, u_k) - F_{\text{R}}(s_k, v_k)}{M} \right), \end{cases} \quad (1)$$

where $v \in \mathbb{R}$ is the train speed and $u \in \mathbb{R}$ is the input handle such that $\forall k \in \mathbb{N}_0$ it holds

$$v_k \in \mathcal{V}(s), \quad (2a)$$

$$u_k \in \mathcal{U}, \quad (2b)$$

with $\mathcal{V}(s) := [0, \bar{v}(s)]$, and $\bar{v}(s) > 0$ being the maximum allowed velocity depending on train position, and $\mathcal{U} := [-1, 1]$. Note that, for the sake of simplicity, the time index k is omitted in the following. The traction and braking forces, denoted as $F_T \in \mathbb{R}$ and $F_B \in \mathbb{R}$, are given by

$$F_T(v, u) = \overline{F}_T(v) u, \tag{3a}$$
$$F_B(v, u) = \overline{F}_B(v) u, \tag{3b}$$

where $\overline{F}_T \in \mathbb{R}$ and $\overline{F}_B \in \mathbb{R}$ are the maximum traction and braking forces curves depending on the train speed (see Appendix A). The resistance force $F_R \in \mathbb{R}$ is instead given by

$$F_R(s, v) = R_g(s) + R_v(v) \operatorname{step}(v), \tag{4a}$$
$$R_g(s) = M \left(g \tan(\alpha(s)) + \frac{\beta}{r(s)} \right), \tag{4b}$$
$$R_v(v) = A + Bv + Cv^2, \tag{4c}$$

where A, B, C are the so-called *Davis* parameters, g is the gravity acceleration, and β is a specific constant of the train. Note that the resistance component $R_v(v) \operatorname{step}(v)$ is zero when the speed is null, as the train is not travelling.

Electrical model: An equivalent scheme of the train electrical model, equipped with a rheostat, is shown in Fig. 2. In this work we assume that the electrical grid presents reversible substations, so that a partial regenerative braking can take place. A portion of the braking current injected back to the grid can be reused by another train connected to the same substation, while the rest is wasted through the rheostat of the braking train whenever the voltage exceeds a predefined threshold $V_{th} > 0$.
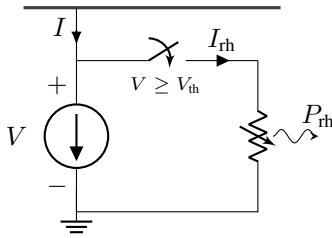

Fig. 2: Electrical circuit model of the train.

The train absorbs the direct current $I \in \mathbb{R}$ from the catenary grid during the traction phase, behaving as a load, while it operates as a current generator during the braking phase. Let us denote with $I_T(v)$ the traction current, and with $I_B(v)$ the braking one, which depends on the train speed as shown in Appendix A. Whenever the train brakes, part of the current $I_B(v)$ flows through the rheostat to avoid an excessive voltage increase on the catenary. Denoting with I_{rh} the current flowing through the rheostat, the dissipated electrical power is

$$P_{rh} = I_{rh} V = \eta_{rh}(V) I_B(v) V, \tag{5}$$

where the fraction value $\eta_{rh} \in [0, 1]$ is

$$\eta_{rh}(V) = \begin{cases} 0, & \text{if } V < V_{th} \\ \frac{V - V_{th}}{\overline{V} - V_{th}} & \text{if } V \geq V_{th} \end{cases}. \tag{6}$$

Therefore, the total current absorbed, or provided, by the train to the catenary grid results in being

$$I = g(v, V, u) = \begin{cases} I_T(v) u, & \text{if } u \geq 0 \\ (1 - \eta_{rh}(V)) I_B(v) u, & \text{if } u < 0 \end{cases}, \tag{7}$$

where the function $g(\cdot)$ is introduced for notational simplicity.

B. Catenary grid model

The catenary grid interface is the most widely used solution in electrical railway systems. In this paper we assume that the catenary grid enables for bidirectional power flow such that traction power is provided to the train when this is in traction mode (i.e., $u \geq 0$), while the braking power is partially converted into electrical power during the so-called regenerative mode (i.e., $u < 0$).

Before describing the overall catenary grid, the model of a short track (typically less than $5\,\mathrm{km}$) with one single substation and one train is firstly presented. The substation can be modelled by a voltage generator, namely $V_s > 0$, while rails and catenary lines can be represented through variable resistors depending on the relative distance of the train with respect to the substation, i.e., $r \cdot s$, with r being the resistance per space of the line. Hence, the train voltage can be written as

$$V = V_s - r \cdot s \cdot I_\ell = V_s - r \cdot s \cdot I, \tag{8}$$

where I_ℓ is the current line, which in this case is equal to I since one substation with one single train is considered.
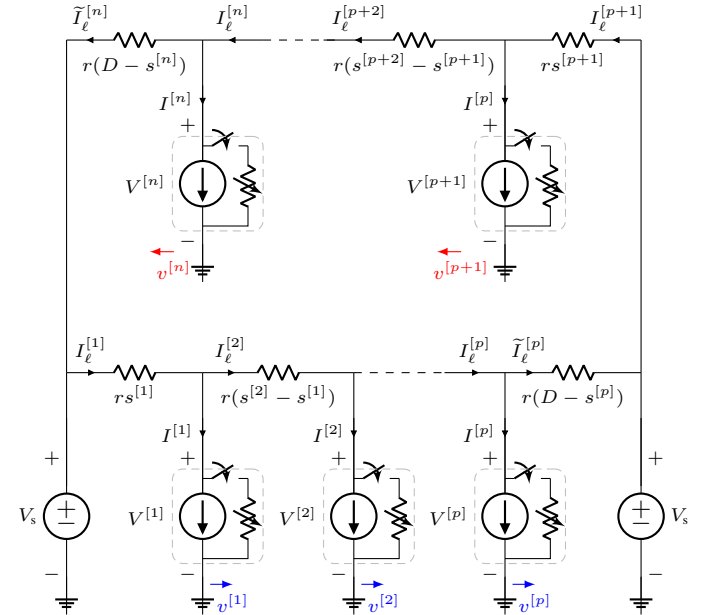

Fig. 3: Bilateral catenary circuit model with p trains in one direction over one track, and $q = n - p$ trains in the opposite direction in another track (see the speed directional arrows).

Consider now the catenary grid in Fig. 3, representing a generic railway scenario. This is electrically supplied from two sides, indicated with voltage generators V_s, which have distance D between each other, giving rise to bilateral electrical substations.

The presented catenary grid comprises n trains travelling in two separate railway tracks, where $p \leq n$ trains travel on one track in a direction and other $q = n - p$ trains travel on the other track in the opposite direction. For the sake of simplicity, it is assumed that, for each track, all trains start their journey from the same initial position and at different time instants $t_0^{[i]}$, where the notation $\cdot^{[i]}$ is used to indicate variables associated to the ith train.

Hence, the sets $\mathcal{P} = \{1, \ldots, p\}$ and $\mathcal{Q} = \{p + 1, \ldots, n\}$ are introduced, where $\mathcal{P}$ includes the sequence of trains in the first track (circuit at the bottom in Fig. 3), while $\mathcal{Q}$ includes the ones in the second track (circuit on the top in Fig. 3). In particular, for each set, trains are numbered in decreasing order with respect to their starting time $t_0^{[i]}$ (i.e., the first train in each set is the last one leaving the initial position of the track). It follows that

$$\mathcal{P} := \{i \in [1, \ldots, p] \quad | \quad t_0^{[i-1]} \geq t_0^{[i]} \; \forall i \in [2, p] \},$$
$$\mathcal{Q} := \{i \in [p + 1, \ldots, n] \quad | \quad t_0^{[i-1]} \geq t_0^{[i]} \; \forall i \in [p + 2, n] \},$$

and the set $\mathcal{N} := \mathcal{P} \cup \mathcal{Q}$ comprises all trains in the two tracks.

At this stage, the overall catenary grid model is presented and the following vectors are introduced

$$\mathbf{V} = [V^{[1]}, \ldots, V^{[n]}]', \tag{9}$$

$$\mathbf{I} = [I^{[1]}, \ldots, I^{[n]}]', \tag{10}$$

$$\mathbf{I}_\ell = [I_\ell^{[1]}, \ldots, I_\ell^{[p]}, \widetilde{I}_\ell^{[p]}, I_\ell^{[p+1]}, \ldots, I_\ell^{[n]}, \widetilde{I}_\ell^{[n]}]', \tag{11}$$

where $\mathbf{V}$, $\mathbf{I}$ and $\mathbf{I}_\ell$ comprise train voltages, currents and the catenary line currents, respectively (see Fig. 3). By applying the *Kirchhoff* laws, the catenary grid model is described as

$$G(s^{[1]}, \ldots, s^{[n]}) \cdot \begin{bmatrix} \mathbf{V} \\ \mathbf{I}_\ell \end{bmatrix} = c\,(V_s, \mathbf{I}), \tag{12}$$

where

$$c\,(V_s, \mathbf{I}) = [\, V_s, \underbrace{0, \ldots, 0}_{p-1}, -V_s, V_s, \underbrace{0, \ldots, 0}_{q-1}, -V_s, \mathbf{I}' \,],$$

and $G(s^{[1]}, \ldots, s^{[n]}) \in \mathbb{R}^{2n+2 \times 2n+2}$ is a matrix function that can be written as

$$G(s^{[1]}, \ldots, s^{[n]}) = \left[\begin{array}{c:c} E & L(s^{[1]}, \ldots, s^{[n]}) \\ \hdashline \mathbf{0}_{n,n} & E' \end{array} \right]. \tag{13}$$

The matrix $E \in \mathbb{R}^{n+2 \times n}$ in (13) can be written as

$$E = \left[\begin{array}{c:c} P & \mathbf{0}_{p+1,q} \\ \hdashline \mathbf{0}_{q+1,p} & Q \end{array} \right],$$

where the matrices $P \in \mathbb{R}^{p+1 \times p}$ and $Q \in \mathbb{R}^{q+1 \times q}$ have elements

$$[P]_{i,j} = \begin{cases} 1 & \text{if } i = j \\ -1 & \text{if } i = j + 1 \,, \\ 0 & \text{otherwise} \end{cases} \quad [Q]_{i,j} = \begin{cases} 1 & \text{if } i = j \\ -1 & \text{if } i = j + 1 \,. \\ 0 & \text{otherwise} \end{cases}$$

On the other hand, L in (13) is a diagonal matrix comprising all catenary resistances, which depend on the distance covered by trains. Thus, introducing the auxiliary vectors $\boldsymbol{\rho}$ and $\boldsymbol{\phi}$, i.e.,

$$\boldsymbol{\rho} = [\, 0, \; s^{[1]}, \ldots, s^{[p]}, \, D \,]',$$
$$\boldsymbol{\phi} = [\, \underbrace{0, \ldots, 0}_{p+2}, \; s^{[p+1]}, \ldots, s^{[n]}, \, D \,]',$$

the elements of the matrix $L(s^{[1]}, \ldots, s^{[n]}) \in \mathbb{R}^{n+2 \times n+2}$ are defined as

$$[L]_{i,j} = \begin{cases} r\,(\rho_{j+1} - \rho_i) & \text{if } i = j \wedge i \in \{1, ..., p+1\} \\ r\,(\phi_{j+1} - \phi_i) & \text{if } i = j \wedge i \in \{p+2, ..., n+2\} \,. \\ 0 & \text{if } i \neq j \end{cases}$$

Note that, in the case of multiple trains, catenary line resistances depend of the distance between consecutive trains in each railway track, and therefore they vary overtime.

C. Single train eco-drive control problem

Now, let us introduce the eco-drive control problem aimed at minimizing the energy consumption of each ith train, while fulfilling the constraints (2), and making the train arrive at the final station at a prescribed time instant $t_f^{[i]}$. As this problem is independently applied to each train, the notation $\cdot^{[i]}$ is here omitted. The eco-drive problem consists in minimizing the discretized integral of the square value of the train acceleration in traction

$$a_k = \frac{F_T(v_k, u_k) - F_R(s_k, v_k)}{M},$$

normalized by its maximum value

$$\bar{a}_k = \frac{\overline{F}_T(v_k) - F_R(s_k, v_k)}{M}.$$

Therefore, it follows that

$$\min_{u_k} J = \sum_{k=k_0}^{k_f} \left(\frac{F_T(v_k, u_k) - F_R(s_k, v_k)}{\overline{F}_T(v_k) - F_R(s_k, v_k)} \right)^2 \tag{14a}$$

subject to, $\forall k \in [k_0, k_f]$,

$$\begin{bmatrix} s_{k+1} \\ v_{k+1} \end{bmatrix} = f(s_k, v_k, u_k), \tag{14b}$$

$$\begin{bmatrix} s_{k_0} \\ v_{k_0} \end{bmatrix} = \begin{bmatrix} 0 \\ 0 \end{bmatrix}, \tag{14c}$$

$$\begin{bmatrix} s_{k_f} \\ v_{k_f} \end{bmatrix} = \begin{bmatrix} s_f \\ 0 \end{bmatrix}, \tag{14d}$$

$$v_k \in \mathcal{V}, \; u_k \in \mathcal{U}, \tag{14e}$$

where $k_0 := \left\lfloor \frac{t_0}{T} \right\rfloor$ and $k_f := \left\lfloor \frac{t_f}{T} \right\rfloor$ are the initial and the final time step of the train journey, respectively, while $f(s_k, v_k, u_k)$ represents the system dynamics (1) under (3)–(4).

Remark 2.1 (Comfortability): It is worth noticing that problem (14) does not only enable to reduce train energy consumption, but it is also beneficial from passengers perspective, as their comfort is much higher when accelerations are reduced.

The problem stated in (14) is a nonlinear control problem characterized by high computational complexity, as the whole travel time horizon k_f is considered and the problem is non-convex, e.g., considering (3)–(4). On the other hand, each train is independently optimized in (14), and the joint coordination

of multiple trains to maximize the overall energy efficiency and minimize electrical grid losses is not addressed. Therefore, alternative efficient control strategies are hereafter proposed.

III. PROPOSED SWITCHING PREDICTIVE CONTROL

Having in mind DAS trains, a quantization of the input handle is needed to make human assistance easier, meaning that, instead of inputs taking any value in a connected compact set, the proposed predictive controller will suggest to the driver one out of a finite discrete set of possible driving modes. Since $m = 4$ operation modes can be used to capture the dynamics of the train [3], as depicted in Fig. 4, the input handle can be accordingly quantized.
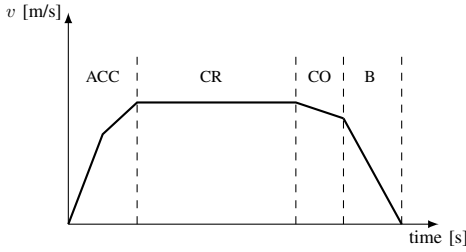

Fig. 4: Train speed profile and motion modes: (ACC) acceleration, (CR) cruising, (CO) coasting, and (B) braking.

The considered train motion modes and the corresponding values of the input handle used in (3), provided by Alstom rail transport relying on data analysis and computational insights in field, are: *i)* acceleration (ACC) mode, where the handle can assume two values $u \in \{0.5, 1\}$, selected by the optimizer in order to enable more flexibility for energy savings over all the track; *ii)* cruising (CR) mode, where the train travels at constant speed, thus the input handle is properly selected, as $u = u_{\mathrm{cr}}$; *iii)* coasting (CO) mode, where the traction force is null and so $u = 0$; *iv)* braking (BR) mode, where the maximum braking force is assumed to be selected for safety reason, i.e., $u = -1$, see (3b). In particular, to maintain constant speed in cruising mode, the input handle $u = u_{\mathrm{cr}}$ is automatically computed by an inner control loop ensuring that $F_{\mathrm{T}} = F_{\mathrm{R}}$ for positive slopes, and $F_{\mathrm{B}} = F_{\mathrm{R}}$ for negative slopes.

Therefore, introducing the switching signal $\sigma_k \in \Sigma = \{1, \ldots, 5\}$ and the set $\mathcal{U}_{\mathrm{sw}} = \{0.5, 1, u_{\mathrm{cr}}, 0, -1\}$, the input handle $u_k(\sigma_k) \in \mathcal{U}_{\mathrm{sw}}$ can be modelled as a switching input. This enables to reformulate the train dynamic model (14b) as a switched system, i.e.,

$$\begin{bmatrix} s_{k+1} \\ v_{k+1} \end{bmatrix} = f(s_k, v_k, u_k(\sigma_k)), \qquad (15)$$

where f is a nonlinear function due to train forces dependency on speed and position (3)–(4).

Using (15) for the train dynamic model, (14) becomes a switching control problem where the integer variable σ_k, $\forall k \in [k_0, k_{\mathrm{f}}]$, must be optimized, eventually defining the optimal values of the input handle suggested by the DAS. Nevertheless, this can be still not a practical approach as the whole train travel time is considered in (14), possibly leading to computational-intensive problem solutions. To overcome this issue, a switching predictive control strategy exploiting the receding horizon approach is hereafter proposed.

A. SNMPC for the single train eco-drive problem

A SNMPC control problem is formulated to be solved at each time instant $k \in \mathbb{N}_0$. The adopted prediction horizon is defined as $\mathcal{T}_k := \{k, \ldots, k + N - 1\} \cap \{k_0, \ldots, k_f\}$, with the integer $N \geq 1$, so as to exclude the time instants out of the train journey in the SNMPC problem. For the sake of notational compactness, let us introduce $N_k := \min(k_{\mathrm{f}} - k, N)$, so that $k + N_k - 1$ is always the final time step in $\mathcal{T}_k$. In the following, the index t is used to span along the prediction horizon, i.e., $t \in \mathcal{T}_k$.

Since a finite prediction horizon $\mathcal{T}_k$ is considered, the final constraint on the position cannot be imposed, i.e., $s_{k_f} = s_f$ in (14d). Hence, this is relaxed and included as an additional term in the SNMPC cost function. This is defined as

$$J_k = \sum_{t \in \mathcal{T}_k} \Bigg((1 - \gamma)\, l(s_t, v_t, u_t(\sigma_t)) + $$
$$+ \gamma_u\, w\big(u_t(\sigma_t), u_{t-1}(\sigma_{t-1})\big) \Bigg) + \gamma\, \xi(s_{k+N_k}), \qquad (16)$$

where

$$l(s_t, v_t, u_t(\sigma_t)) = \left(\frac{\overline{F}_{\mathrm{T}}\, u_t(\sigma_t) - F_{\mathrm{R}}(s_t, v_t)}{\overline{F}_{\mathrm{T}} - F_{\mathrm{R}}(s_t, v_t)} \right)^2,$$

$$w\big(u_t(\sigma_t), u_{t-1}(\sigma_{t-1})\big) = |u_t(\sigma_t) - u_{t-1}(\sigma_{t-1})|,$$

$$\xi(s_{k+N_k}) = \left(\frac{S_k - s_{k+N_k}}{S_k} \right)^2.$$

The first term $l(\cdot)$ in (16) expresses the eco-drive problem cost function (14a), while the second term $w(\cdot)$ is used to avoid unnecessary switching of the input handle, making the human driver assistance easier and improving passengers comfort. The third term $\xi(\cdot)$ in (16) evaluates the final position error with respect to the space horizon S_k, which is a parameter representing the distance that must be travelled over the prediction horizon to guarantee the prescribed arrival time.

Remark 3.1 (Space horizon): The value S_k in $\xi(s_{k+N_k})$ can be computed according to a heuristic procedure. For instance, the train all-out solution (that is the one giving the shortest arrival time compatible with the train parameters and constraints) can be exploited.

The weight $\gamma \in [0, 1]$ in (16) is a tuning parameter, either prioritizing the reduction of train acceleration, and so the absorbed current, or increasing the travelled distance and consequently minimizing the travel time. Introducing $\boldsymbol{\sigma}_k = [\sigma_k, \ldots, \sigma_{k+N_k-1}]'$, the SNMPC formulation for the eco-drive problem is stated as

$$\min_{\boldsymbol{\sigma}_k} J_k$$

subject to, $\forall t \in \mathcal{T}_k$,

$$\begin{bmatrix} s_{t+1} \\ v_{t+1} \end{bmatrix} = f(s_t, v_t, u_t(\sigma_t)), \qquad (17)$$
$$\begin{bmatrix} s_k \\ v_k \end{bmatrix} = \begin{bmatrix} \tilde{s}_k \\ \tilde{v}_k \end{bmatrix}$$

$$v_t \in \mathcal{V}, \quad u_t(\sigma_t) \in \mathcal{U}_{\mathrm{sw}},$$

where $[\tilde{s}_k, \tilde{v}_k]'$ expresses the measured state at each $k \in \mathbb{N}_0$.

The formulated SNMPC problem (17) can be still computational demanding, so that actually further realistic simplifications have to be considered. These have been defined in accordance with the industrial partner Alstom rail transport, which provided the real world test data presented in Appendix A. The adopted simplification guidelines are hereafter reported.

1) Braking distance pre-computation: As the train approaches its final position, it must brake to satisfy the final state condition (14d). In this context, the braking distance D_{BR} can be computed, representing the space needed by the train to go from the actual speed to zero when the braking mode is activated, as depicted in Fig. 5.
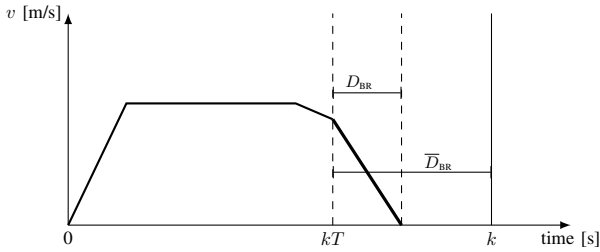

Fig. 5: Rendering of the braking distance pre-computation.

Under the braking condition, the train model (1) becomes an autonomous dynamical system

$$\begin{cases} s_{k+1} &= s_k + T v_k, \\ v_{k+1} &= v_k - T \left(\frac{\overline{F}_{\mathrm{B}}(v_k) + F_{\mathrm{R}}(s_k, v_k)}{M} \right), \end{cases} \quad (18)$$

implying that the state free motion starting from an initial condition $s_k = \tilde{s}_k$, $v_k = \tilde{v}_k$ can be analysed. The number of time steps needed to stop the train, denoted as k_{BR}, can be computed by iterating the speed dynamical equation, i.e.,

$$v_{k+k_{\mathrm{BR}}} = \tilde{v}_k - T \sum_{t=k}^{k+k_{\mathrm{BR}}-1} \frac{\overline{F}_{\mathrm{B}}(v_t) + F_{\mathrm{R}}(s_t, v_t)}{M} = 0, \quad (19)$$

where the state dynamics (18) is recursively substituted in (19). Therefore, exploiting the dynamical equation of the position, the braking distance can be computed as

$$\begin{aligned} D_{\mathrm{BR},k} &= s_{k+k_{\mathrm{BR}}} - \tilde{s}_k = T \sum_{t=k}^{k+k_{\mathrm{BR}}-1} v_t = \\ &= \tilde{v}_k \, k_{\mathrm{BR}} \, T - T^2 \sum_{t=k+1}^{k+k_{\mathrm{BR}}-1} \sum_{l=k}^{t-1} \frac{\overline{F}_{\mathrm{B}}(v_l) + F_{\mathrm{R}}(s_l, v_l)}{M}. \end{aligned} \quad (20)$$

The information on the braking distance can be used to force the train to brake when the remaining distance $\overline{D}_{\mathrm{BR},k} := s_f - \tilde{s}_k$ is equal to or lower than $D_{\mathrm{BR},k}$, as evident from Fig. 5. Introducing the boolean variable $\delta_{\mathrm{BR},k}$, defined as $\delta_{\mathrm{BR},k} = 1$ if $D_{\mathrm{BR},k} \geq \overline{D}_{\mathrm{BR},k}$, the following constraints can be included to (17) to force the braking mode

$$\overline{D}_{\mathrm{BR},t} - D_{\mathrm{BR},t} \geq \epsilon - (H + \epsilon) \delta_{\mathrm{BR},t}, \quad (21a)$$

$$-1 \leq u_t(\sigma_t) \leq -1 + (1 - \delta_{\mathrm{BR},t}) H, \quad (21b)$$

where $t \in \mathcal{T}_k$, $\epsilon > 0$ in (21a) is chosen as a very small number, while $H \gg 0$ in (21) as a very large one [25].

The braking distance $D_{\mathrm{BR},k}$ is also analysed at each $k \in \mathbb{N}_0$, right before executing the SNMPC problem (17). In fact, in case $D_{\mathrm{BR},k} \geq \overline{D}_{\mathrm{BR},k}$, the problem (17) is avoided to be solved and the braking mode is directly forced, posing $u_k(\sigma_k) = -1$ until the train stops.

2) Switching rules: The optimal input sequence obtained by (17), denoted as $\mathbf{u}_k^* = [u_k^*(\sigma_k^*), \dots, u_{k+N_k-1}^*(\sigma_{k+N_k-1}^*)]$, is contained in the set of all possible input sequences $\mathcal{W}$, where in particular $|\mathcal{W}| = (m+1)^{N_k}$. This number is strictly related to the computational complexity of (17), and it can become very large in presence of large prediction horizons. To overcome this issue, switching rules are introduced, reducing the set of feasible input sequences, i.e., $\mathbf{u}_k^* \in \mathcal{F} \subset \mathcal{W}$. The latter are determined relying on driving data analysis in field, so that the permitted switchings between modes are those described by the finite state machine diagram depicted in Fig. 6. In particular, it is imposed that: *i)* a direct transition between the acceleration and the braking mode cannot occur; *ii)* a direct transition from the braking mode to the cruising mode cannot occur; *iii)* apart from the medium acceleration mode ($u = 0.5$), a direct transition between the maximum acceleration mode ($u = 1$) and any other mode cannot occur. The switching rules can be easily implemented as mixed-integer linear constraints using techniques discussed in [25].
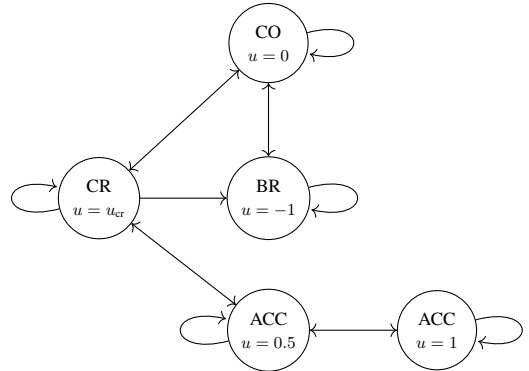

Fig. 6: Finite state machine for the considered switching rules.

3) Move-blocking strategy: To further reduce the computational burden of the algorithm, the move-blocking parametrization approach can be adopted [26]. According to this strategy, the input variables are constrained to vary at each N_u steps along the prediction horizon, instead of at each time instant, where $1 < N_u < N$. This approach can drastically reduce the set of possible input sequences, and so the computational complexity, still being able to vary the input at any time instant as (17) is solved at each $k \in \mathbb{N}_0$.

The eco-drive control problem presented in (14), solved through the SNMPC strategy in (17), considers the energy consumption minimization of each single train, without taking into account the overall system. Nevertheless, as described in Section II-B, multiple trains supplied by the same power line are all electrically connected. This means that their joint operation can be controlled so as to maximize the energy efficiency of the overall railway system.
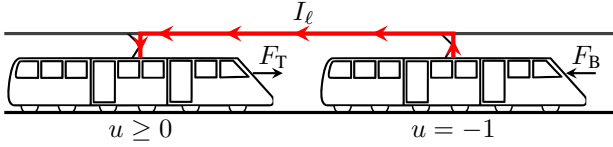
Fig. 7: Principle of collaborative eco-drive for $n = 2$ trains.

In particular, energy dissipations in catenary lines and in train rheostats can be minimized by coordinating the operation modes of the multiple trains. As an example, the regenerative energy recovered by a train while braking, instead of being passively transferred to the substations or dissipated by the rheostat, can be re-used by the "closest" train connected to the grid through its synchronous activation of the acceleration mode, as shown in Fig. 7. This joint coordination will have the beneficial effect of minimizing energy losses in railway systems, still enabling trains to arrive to their destinations in pre-scribed time. To accomplish this task, a collaborative control strategy is designed and presented in the following.

B. SNMPC for collaborative eco-drive

The collaborative control strategy involves the joint optimization of the operations of all trains in $\mathcal{N}$, always according to a SNMPC approach, solved at each $k \in \mathbb{N}_0$. In particular, each ith train is characterized by its own prediction horizon considering the initial and final instants, i.e., $\mathcal{T}_k^{[i]} := \{k, \dots, k + N - 1\} \cap \{k_0^{[i]}, \dots, k_f^{[i]}\}$, with $N \geq 1$ and $N_k^{[i]} = \min(k_f^{[i]} - k, N)$. The maximum prediction horizon is also introduced and defined as $\overline{\mathcal{T}}_k := \bigcup_{\forall i \in \mathcal{N}} \mathcal{T}_k^{[i]}$.

As mentioned, the control problem presented in this section enables not only to optimize energy exchanges between trains, but also to reduce electrical power losses. Therefore, the cost function $J_t^\dagger$ related to each ith train is defined as

$$
\begin{aligned}
J_t^{\dagger\,[i]} = \sum_{t \in \mathcal{T}_k^{[i]}} \Bigg(& (1 - \gamma_k^{[i]})\, l(s_t^{[i]}, v_t^{[i]}, u_t^{[i]}(\sigma_t^{[i]})) + \\
& + \gamma_u^{[i]}\, w\big(u_t^{[i]}(\sigma_t^{[i]}), u_{t-1}^{[i]}(\sigma_{t-1}^{[i]})\big) \Bigg) + \gamma_k^{[i]}\, \xi(s_{k+N_k}) + \\
& + \sum_{t \in \mathcal{T}_k^{[i]}} \eta_{\mathrm{rh}}(V_t^{[i]}) I_{\mathrm{B}}^{[i]}(v_v^{[i]}) V_t^{[i]},
\end{aligned}
\tag{22}
$$

where the first terms are defined as in (16), while the last term comprises the rheostat power losses. Note also that the weight γ_k is now time-varying, as it will be optimized at each $k \in \mathbb{N}_0$ to enhance the collaboration between trains.

The SNMPC problem for collaborative trains is stated as

$$
\min_{\substack{\boldsymbol{\sigma}_k^{[1]}, \dots, \boldsymbol{\sigma}_k^{[n]} \\ \gamma_k^{[1]}, \dots, \gamma_k^{[n]}}} \quad \sum_{\forall i \in \mathcal{N}} J_t^{\dagger\,[i]} + \gamma_\ell \sum_{t \in \overline{\mathcal{T}}_k} \mathbf{I}_{\ell,t}^{'} L_t \mathbf{I}_{\ell,t}
\tag{23a}
$$

subject to, $\forall t \in \overline{\mathcal{T}}_k$ and $\forall i \in \mathcal{N}$,

$$
\begin{bmatrix} s_{t+1}^{[i]} \\ v_{t+1}^{[i]} \end{bmatrix} = f\big(s_t^{[i]}, v_t^{[i]}, u_t^{[i]}(\sigma_t^{[i]})\big),
\tag{23b}
$$

$$
\begin{bmatrix} s_k^{[i]} \\ v_k^{[i]} \end{bmatrix} = \begin{bmatrix} \tilde{s}_k^{[i]} \\ \tilde{v}_k^{[i]} \end{bmatrix},
\tag{23c}
$$

$$
I_t^{[i]} = g\big(v_t^{[i]}, V_t^{[i]}, u_t^{[i]}(\sigma_t^{[i]})\big),
\tag{23d}
$$

$$
v_t^{[i]} \in \mathcal{V},
\tag{23e}
$$

$$
u_t^{[i]}(\sigma_t^{[i]}) \in \mathcal{U}_{\mathrm{sw}},
\tag{23f}
$$

$$
u_t^{[i]}(\sigma_t^{[i]}) = 0 \qquad \forall t \notin [k_0^{[i]}, k_f^{[i]}],
\tag{23g}
$$

$$
\gamma_k^{[i]} \in \Gamma \subseteq [0,1],
\tag{23h}
$$

$$
G(s_t^{[1]}, \dots, s_t^{[n]}) \cdot \begin{bmatrix} \mathbf{V}_t \\ \mathbf{I}_{\ell,t} \end{bmatrix} = c\,(V_{\mathrm{s}}, \mathbf{I}_t).
\tag{23i}
$$

The cost function (23a) aims at minimizing trains local cost functions and the power losses in the catenary grid weighted by γ_ℓ. The latter are computed through the resistance matrix L_t and the line currents, modelled in (23i) as described in Section II-B. Among the constraints, the dynamical and electrical train models are considered in (23b)-(23d), the local train constraints in (23e)-(23f), while (23g) avoids to optimize trains out of their starting and arrival time. Finally, (23h) is also included, as $\gamma_k^{[i]}$ is now an optimization variable, where $\Gamma \subseteq [0,1]$ is a suitably chosen finite set to limit the computational burden.

The variable $\gamma_k^{[i]}$ in (23) plays a crucial role in the collaborative control strategy, being it optimized to prioritize either the minimization of the train acceleration or the remaining space distance. In particular, low values of $\gamma_k^{[i]}$ makes the train slow down (i.e., less energy is required), while high values of $\gamma_k^{[i]}$ makes the train accelerate (i.e., more energy is absorbed from the catenary grid). The objective of the optimal control problem (23) is actually to coordinate these operations, meanwhile minimizing the overall losses in the catenary. Considering the example shown in Fig. 7, as the second train starts to brake, injecting energy in the catenary grid, the proposed SNMPC determines an increase of $\gamma_k^{[1]}$ for the first train, so as to reduce its weight of the acceleration term, exploiting the energy regenerated by the second train.

Remark 3.2 (Practical feasibility): According to a preliminary feasibility study of the proposal, the solution to the SNMPC problem (23) can be computed in correspondence of the substations which trains share during their journey. It is indeed physically reasonable to assume any substation equipped with the needed computational power and capable of receiving data from and sending data to trains, which can in turn communicate any information among each other.

IV. CASE STUDY

In this section, the proposed SNMPC is assessed in simulation relying on realistic scenarios based on real data, provided by Alstom rail transport.

A. Settings

The simulated test benchmark consists of two scenarios with 2 stops and bilateral ESS, one placed at the departure station and the other in correspondence of the second stop. The first scenario represents an illustrative case study with $n = p = 2$ (i.e., only one track) metro trains, in order to clearly show the concept of collaboration between trains and the advantages of the proposed SNMPC approach. Then, a more complex and realistic scenario is also reported. The latter involves $n = 7$ metro trains, with $p = 4$ trains in one track, and $q = 3$ trains on the other track in opposite direction. The parameters of the tracks, of the trains and of the catenary grid are reported in Appendix A. The proposed SNMPC is designed by considering a sampling time $T = 1$ s and horizon $N = 10$. The weight on the variation of the input handle (see (22)) is chosen as $\gamma_u^{[i]} = 0.005$, $\forall i \in \mathcal{N}$, while $\Gamma = \{0.85, 0.98\}$. This set has been defined after a tuning procedure, choosing its minimum value to fulfil travel time requirements (the smaller $\gamma_k^{[i]}$, the smaller the weight on the final position), and its maximum value being slightly lower than 1 to never neglect the acceleration term in (22).

B. Results on the 2-trains scenario

Consider now the case of $n = p = 2$ trains. According to the proposed control logic, the speed profiles of the two trains are depicted in Fig. 8. As expected, the two trains complete their journey in prescribed times, each of them starting at a different $k_0^{[i]}$. Moreover, despite the relaxation of the final state constraint (14d), the trains travel the required distance to reach the final stops, as reported in Fig. 9.
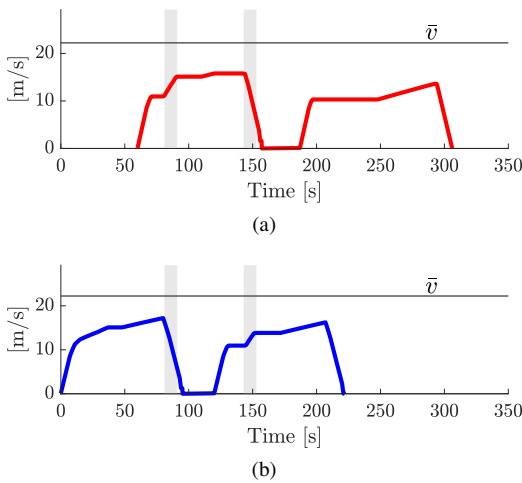
Fig. 8: Speed profiles in collaborative mode for train 1 (a) and train 2 (b). Shadow areas identify time instants where trains collaboration occurs.
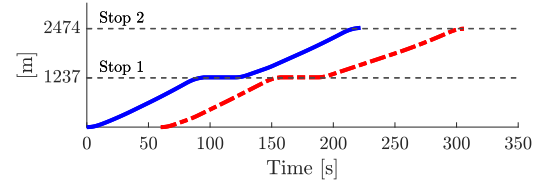
Fig. 9: Travelled distance profiles for train 1 (dashed red) and train 2 (solid blue).

The collaborative behaviour induced by the proposed SN-MPC is also evident from Fig. 8. In fact, during the braking phase of each train in correspondence of the first stop, one has that the other train starts to accelerate, thus exploiting the regenerated energy. The shadow windows in Fig. 8 highlight such phases. It is worth highlighting that when train $i = 2$ brakes between 210 and 225 s, train $i = 1$ does not exploit the regenerated energy to accelerate, that is no collaboration occurs. This happens because, in that time interval, train $i = 2$ is closer to the ESS placed at the second stop rather than to train $i = 1$, as evident also from Fig. 9, and the collaboration between the two trains would imply higher line losses.

The value of $\gamma_k^{[i]}$ is adapted by the SNMPC to enhance such a collaboration, as depicted in Fig. 10. In fact, during the collaborative phases (shadow windows in Fig. 10), the weight $\gamma_k^{[i]}$ is optimized so as to reach its highest value in Γ, thus inducing the ith train to accelerate and recover the regenerated braking energy. The corresponding voltage profiles are depicted in Fig. 11. In particular, it is possible to observe that voltages are kept below the voltage threshold V_{th} by virtue of the rheostat current absorption, thus limiting the current flowing and the voltage drops along the catenary. Finally, note that the proposed SNMPC has been tested on a laptop with Intel Core i7-11850H processor, achieving an average computational time of 0.03 s to solve (23).
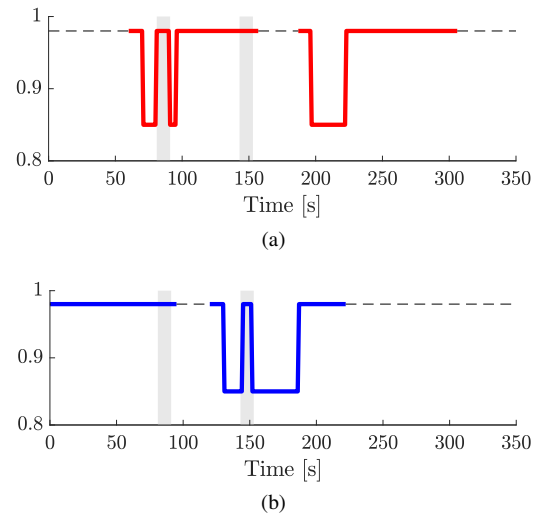
Fig. 10: Optimal values of $\gamma_k^{[i]}$ in collaborative mode for train 1 (a) and train 2 (b). Shadow areas identify time instants where trains collaboration occurs. Dashed lines do not represent significant values of $\gamma_k^{[i]}$ since trains are not travelling there.
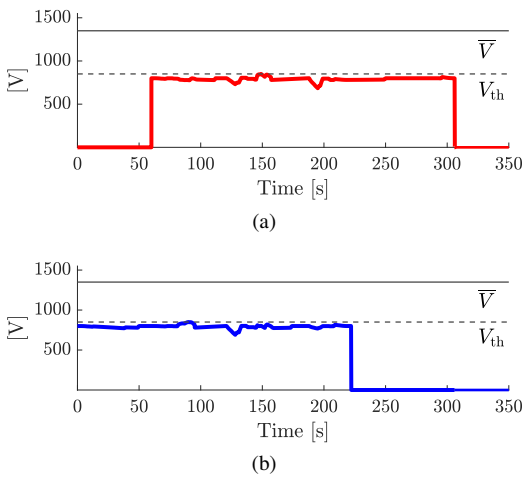
Fig. 11: Voltage profiles in collaborative mode for train 1 (a) and train 2 (b).

Comparison and discussion: In order to further assess the proposed collaborative eco-drive (briefly, C-eco) strategy, a comparison with the corresponding non-collaborative (briefly, NC-eco) counterpart is performed. The latter is meant as the solution to the optimization problem (17), solved independently for each train. In particular, the value of $\gamma^{[i]}$ is kept constant in (17) and set equal to $\gamma^{[i]} = 0.98 \in \Gamma$, $\forall i \in \mathcal{N}$, to fulfil the travel time requirements.

In Fig. 12, it is evident that trains controlled via the NC-eco strategy accomplish their journey in prescribed time, without any interaction between each other (note that the two speed profiles are identical). Such a behaviour corresponds to higher line losses in the catenary grid, since all regenerative power is transferred to the substations or wasted through the rheostat instead of being directly shared between trains. On the other hand, it is evident that the total travel time increases in the case of C-eco strategy, as visible also in Fig. 13, where the catenary voltages, whose magnitude is comparable for the two optimization-based approaches, are illustrated.
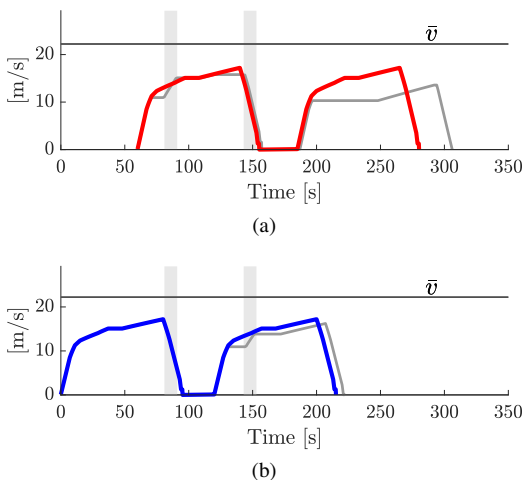

Fig. 12: Speed profiles in non-collaborative mode with respect to the ones in collaborative mode (gray lines), for train 1 (a) and train 2 (b).
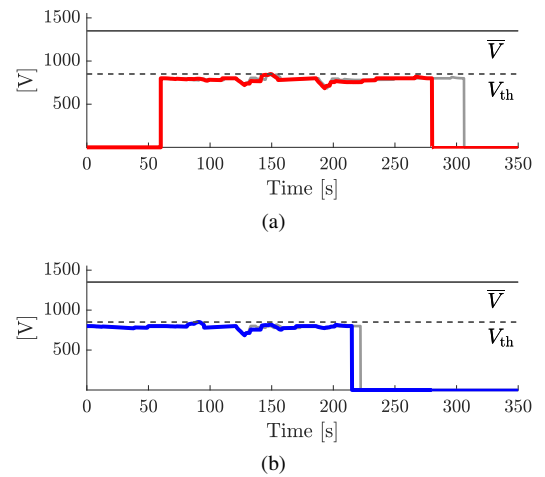

Fig. 13: Voltage profiles in non-collaborative mode with respect to the ones in collaborative mode (gray lines), for train 1 (a) and train 2 (b).

Finally, the outcomes of the simulation campaign in terms of provided energy from the substations, catenary line losses, rheostat losses and average travel time for each stop are reported in Table I.

TABLE I: Performance indexes in the 2-trains scenario.

Indexes	NC-eco ($\gamma^{[i]} = 0.98$)	C-eco	$\Delta_\%$
Absorbed energy [kWh]	22.4	19.8	-11.6%
Line losses [kWh]	1.8	1.5	- 16.7%
Rheostat losses [kWh]	4.1	2.6	-36.6%
Average travel time [s]	217.5	234	+8%

It is worth noticing that high energy savings are achieved by the collaborative eco-drive at the price of a higher (8%) average travel time. Specifically, if on the one hand, a 11.6% and 16.7% reduction are achieved in terms of energy supplied by the substations and energy saved from lines, respectively, a much higher amount of energy is saved from rheostat power losses, i.e., 36.6%. The results confirm the expected benefits due to the energy exchange conditions between trains.

Remark 4.1 (Travel time): As evident from Table I, the NC-eco solution allows a shorter travel time with respect to the C-eco strategy, thus leading to higher energy consumption. The NC-eco solution has been also simulated with $\gamma^{[i]} = 0.97, \forall i \in \mathcal{N}$ to achieve the same travel time obtained by using the C-eco strategy. As evident from Table II, even with the same travel time, the C-eco strategy is still more convenient with respect to NC-eco one in terms of energy consumption.

TABLE II: Performance indexes in the 2-trains scenario with equal travel time for the NC-eco and the C-eco strategies.

Indexes	NC-eco ($\gamma^{[i]} = 0.97$)	C-eco	$\Delta_\%$
Absorbed energy [kWh]	21	19.8	-5.7%
Line losses [kWh]	1.5	1.5	0%
Rheostat losses [kWh]	3	2.6	-13.3%
Average travel time [s]	234	234	0%

C. Results on the 7-trains scenario

In order to assess the scalability of the proposal in a more complex scenario, the case of $n = 7$ trains is now discussed.
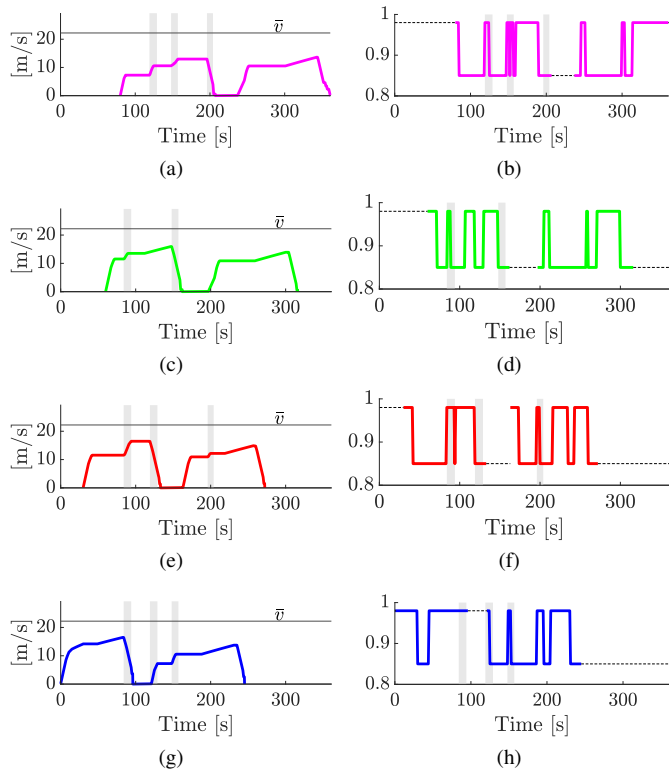

Fig. 14: Speed profiles (left) and optimal values of $\gamma_k^{[i]}$ (right) in collaborative mode for $p = 4$ trains on the first track. Shadow areas identify time instants where trains collaboration occurs.
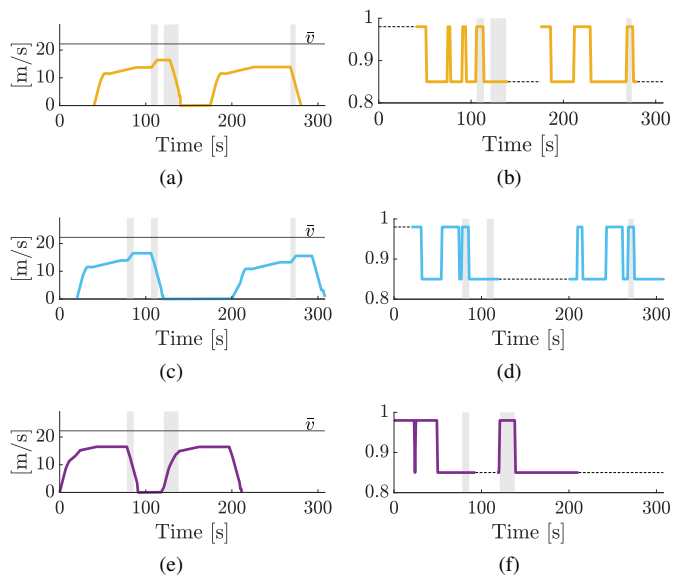

Fig. 15: Speed profiles (left) and optimal values of $\gamma_k^{[i]}$ (right) in collaborative mode for $q = 3$ trains on the second track. Shadow areas identify time instants where trains collaboration occurs.

Figs. 14 and 15 on the left show the speed profiles of the $p = 4$ trains travelling on the first track, and of the $q = 3$ trains moving on the other track, respectively. Note that the three trains in the second track move in the opposite direction and, as a consequence, the optimization takes accordingly into account the track profile. As in the 2-trains scenario, also in this case the proposed SNMPC induces a collaborative behaviour highlighted by the shadow windows in the figures. This collaboration is enhanced by the adaptation of the weight $\gamma_k^{[i]}$, which reaches the highest value during the collaboration phases, as reported in Figs. 14 and 15 on the right.

It is worth highlighting that, despite the increased number of trains in a more complex scenario, the solution to the proposed SNMPC is still feasible with an average computational time of 0.17 s to solve (23). Clearly, as expected, the computation time rises with the higher number of trains. Yet, even with the most demanding settings, the average computation time for the SNMPC is below $T = 1$ s. Note that, due to the catenary grid configuration, the proposal could be further sped up via parallelization, thus allowing to linearly scale the proposed algorithm computations with the number of tracks.

Comparison and discussion: The proposed collaborative eco-drive strategy in this larger scale scenario is again compared with the corresponding non-collaborative counterpart. The same performance indexes adopted for the 2-trains scenario are hereafter provided in Table III.

TABLE III: Performance indexes in the 7-trains scenario.

Indexes	NC-eco	C-eco	$\Delta_\%$
Absorbed energy [kWh]	77.9	72	-7.6%
Line losses [kWh]	5.9	4.6	-22.5%
Rheostat losses [kWh]	10.8	1.8	-83.6%
Average travel time [s]	224	252	12.5%

Analogously to the previous case, high energy savings are achieved by the collaborative eco-drive. Although a higher average travel time is evident (less than 30 s) for the collaborative approach, a 7.6% reduction is achieved in terms of energy supplied by the substations, a 22.5% of energy is saved from lines, and a 83.6% of energy is saved from rheostat power losses, thus again confirming the beneficial effects due to the energy exchange among trains.

V. CONCLUSIONS

In this paper, a novel energy-efficient train control strategy is proposed based on a SNMPC tailored to enhance eco-driving in a collaborative fashion among all the trains connected to the catenary grids. The proposed approach exploits the potential of prediction based recursive online optimization for minimizing the energy consumption of the trains, contemporarily taking into account power line losses, and guaranteeing constraints satisfaction on speed limits and arrival times. Moreover, the proposal is designed to meet specific requirements that make the implementation for DAS trains possible, where the human driver could easily select the input sequences provided by the controller. A numerical validation based on a realistic simulation environment and real data is also presented showing the potentiality of the proposed approach.

Future works could be devoted to the development of distributed predictive control approaches for trains without catenary grid, and in presence of storage devices which inevitably imply the introduction of new models and constraints. A future direction could be also that of designing hierarchical collaborative eco-drive control approaches for ATO trains, and the optimization of train time-tables.

VI. Acknowledgements

Appendix A
Case Study Real World Test Data

The following data have been provided by Alstom rail transport, relying on real world test cases.

The parameters of the catenary grid and the metro trains used for the case study described in Section IV are reported in Table IV. The trains are simulated to reach two consecutive stops in the same track. The track length to reach the first stop from the initial position, and the one to reach the second stop from the first one, is the same, i.e., $S_f = 1237$ m. The slope along the track, i.e., $\alpha(s)$, is depicted in Fig. 16, while the curvature radius is $r(s) = 0, \forall s \in [0, 2\,S_f]$. The maximum traction and braking force curves of the trains, i.e., $\overline{F}_T(v)$ and $\overline{F}_B(v)$, are depicted in Fig. 17(a), while the traction and braking currents i.e., $I_T(v)$ and $I_B(v)$, are depicted in Fig. 17(b). The start and arrival times for the 2-train and the 7-train scenarios are reported in Table V.

Finally, with the objective of reducing the computational complexity of the SNMPC problem, a reduced set of feasible handle sequences is considered, according to pre-defined subset of switching rules provided by Alstom rail transport, which are reported in Table VI.

TABLE IV: Parameters of the trains and of the catenary grid.

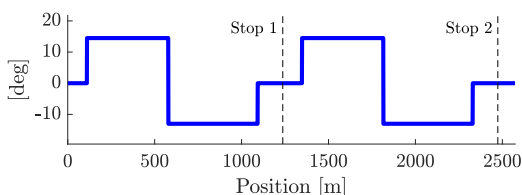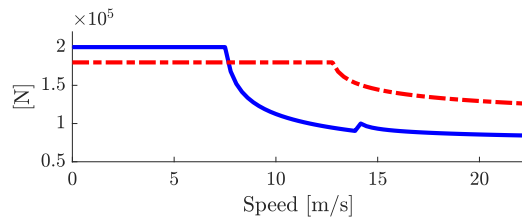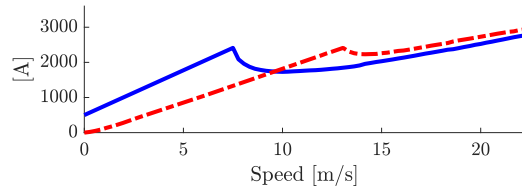|	Trains			Catenary grid	
M	163403	kg	D	2500	m
A	3597.6	N	r	$8e^{-5}$	Ωm^{-1}
B	119.51	Nm^{-1}	V_s	800	V
C	6.9608	Ns^2m^{-1}	V_{th}	850	V
β	800	Nm	$\overline{V}$	930	V

Fig. 16: Slope $\alpha(s)$ along the considered track with two stops.

(a)

(b)

Fig. 17: Maximum traction (solid blue) and braking (dashed red) force curves, i.e., $\overline{F}_T(v)$ and $\overline{F}_B(v)$, respectively (a). Traction (solid blue) and braking (dashed red) current curves, i.e., $I_T(v)$ and $I_B(v)$, respectively (b).

TABLE V: Starting and arrival times for the 2 stops journey.

2-trains scenario				2-trains scenario		
Stop 1	$t_0^{[i]}$ [s]	$t_f^{[i]}$ [s]		Stop 2	$t_0^{[i]}$ [s]	$t_f^{[i]}$ [s]
Train 1	65	180		Train 1	205	320
Train 2	0	115		Train 2	140	255

7-trains scenario				7-trains scenario		
Stop 1	$t_0^{[i]}$ [s]	$t_f^{[i]}$ [s]		Stop 2	$t_0^{[i]}$ [s]	$t_f^{[i]}$ [s]
Train 1	80	215		Train 1	237	370
Train 2	60	165		Train 2	197	320
Train 3	30	140		Train 3	163	280
Train 4	0	105		Train 4	120	250
Train 5	40	145		Train 5	175	290
Train 6	20	125		Train 6	200	315
Train 7	0	110		Train 7	118	220

TABLE VI: Feasible handle sequences for the SNMPC.

	$\mathbf{u}_k \in \mathcal{F} \subset \mathcal{W}$			
#	k	$k+1$	...	$k+N-1$
1	-1	-1	-1	-1
2	0	0	0	0
3	u_{cr}	-1	-1	-1
4	u_{cr}	0.5	0	0
5	1	1	1	1
6	u_{cr}	u_{cr}	u_{cr}	u_{cr}
7	u_{cr}	u_{cr}	0	0
8	u_{cr}	u_{cr}	-1	-1
9	u_{cr}	u_{cr}	0.5	0.5
10	0.5	0.5	0.5	0.5
11	u_{cr}	-1	0	0
12	0	-1	-1	-1
13	-1	-1	0	0
14	-1	0	0	0
15	-1	0.5	0.5	0.5

References

[1] X. Yang, X. Li, B. Ning, and T. Tang, "A survey on energy-efficient train operation for urban rail transit," *IEEE Trans. on Intelligent Transportation Systems*, vol. 17, no. 1, pp. 2–13, 2016.

[2] G. M. Scheepmaker, R. M. Goverde, and L. G. Kroon, "Review of energy-efficient train control and timetabling," *European Journal of Operational Research*, vol. 257, no. 2, pp. 355–376, 2017.

[3] A. Albrecht, P. Howlett, P. Pudney, X. Vu, and P. Zhou, "The key principles of optimal train control–part 1: Formulation of the model, strategies of optimal type, evolutionary lines, location of optimal switching points," *Transp. Research Part B: Methodological*, vol. 94, pp. 482–508, 2016.

[4] G. P. Incremona and P. Polterauer, "Design of a switching nonlinear mpc for emission aware ecodriving," *IEEE Trans. on Intelligent Vehicles*, vol. 8, no. 1, pp. 469–480, 2023.

[5] R. Franke, P. Terwiesch, and M. Meyer, "An algorithm for the optimal control of the driving of trains," in *IEEE 39th Conference on Decision and Control*, Sydney, NSW, Australia, Dec. 2000, pp. 2123–2128.

[6] E. Khmelnitsky, "On an optimal control problem of train operation," *IEEE Trans. on Automatic Control*, vol. 45, no. 7, pp. 1257–1266, 2000.

[7] M. Dominguez, A. Fernández-Cardador, A. P. Cucala, and R. R. Pecharroman, "Energy savings in metropolitan railway substations through regenerative energy recovery and optimal design of ATO speed profiles," *IEEE Trans. on Automation Science and Engineering*, vol. 9, no. 3, pp. 496–504, 2012.

[8] X. Yang, A. Chen, X. Li, B. Ning, and T. Tang, "An energy-efficient scheduling approach to improve the utilization of regenerative energy for metro systems," *Transportation Research Part C: Emerging Technologies*, vol. 57, pp. 13–29, 2015.

[9] A. Nasri, M. F. Moghadam, and H. Mokhtari, "Timetable optimization for maximum usage of regenerative energy of braking in electrical railway systems," in *Int. Symp. on Power Electronics Electrical Drives Automation and Motion*, Pisa, Italy, Jun. 2010, pp. 1218–1221.

[10] M. Peña-Alcaraz, A. Fernández, A. P. Cucala, A. Ramos, and R. R. Pecharromán, "Optimal underground timetable design based on power flow for maximizing the use of regenerative-braking energy," *Journal of Rail and Rapid Transit*, vol. 226, no. 4, pp. 397–408, 2012.

[11] I. Asnis, A. Dmitruk, and N. Osmolovskii, "Solution of the problem of the energetically optimal control of the motion of a train by the maximum principle," *USSR Computational Mathematics and Mathematical Physics*, vol. 25, no. 6, pp. 37–44, 1985.

[12] P. Howlett, "Optimal strategies for the control of a train," *Automatica*, vol. 32, no. 4, pp. 519–532, 1996.

[13] ——, "The optimal control of a train," *Automatica*, vol. 98, pp. 65–87, 2000.

[14] D. Q. Mayne, "Model predictive control: Recent developments and future promise," *Automatica*, vol. 50, no. 12, pp. 2967–2986, 2014.

[15] S. Aradi, T. Bécsi, and P. Gáspár, "A predictive optimization method for energy-optimal speed profile generation for trains," in *IEEE 14th International Symposium on Computational Intelligence and Informatics (CINTI)*, Budapest, Hungary, Nov. 2013, pp. 135–139.

[16] J. C. Geromel and P. Colaneri, "Stability and stabilization of discrete-time switched systems," *International Journal of Control*, vol. 79, no. 7, pp. 719–728, 2006.

[17] P. Mhaskar, N. H. El-Farra, and P. D. Christofides, "Predictive control of switched nonlinear systems with scheduled mode transitions," *IEEE Trans. on Automatic Control*, vol. 50, no. 11, pp. 1670–1680, 2005.

[18] P. Colaneri and R. Scattolini, "Robust model predictive control of discrete-time switched systems," *IFAC Proceedings Volumes*, vol. 40, no. 14, pp. 208–212, 2007.

[19] M. A. Müller and F. Allgöwer, "Improving performance in model predictive control: Switching cost functionals under average dwell-time," *Automatica*, vol. 48, no. 2, pp. 402–409, 2012.

[20] L. Zhang, S. Zhuang, and R. D. Braatz, "Switched model predictive control of switched linear systems: feasibility, stability and robustness," *Automatica*, vol. 67, pp. 8–21, 2016.

[21] H. Farooqi, L. Fagiano, P. Colaneri, and D. Barlini, "Shrinking horizon parametrized predictive control with application to energy-efficient train operation," *Automatica*, vol. 112, p. 108635, 2020.

[22] X. Yan, B. Cai, B. Ning, and W. ShangGuan, "Online distributed cooperative model predictive control of energy-saving trajectory planning for multiple high-speed train movements," *Transportation Research Part C: Emerging Technologies*, vol. 69, pp. 60–78, 2016.

[23] H. Novak, V. Lešić, and M. Vašak, "Hierarchical coordination of trains and traction substation storages for energy cost optimization," in *20th International Conference on Intelligent Transportation Systems*, Yokohama, Japan, Oct. 2017, pp. 1–6.

[24] H. Farooqi, G. P. Incremona, and P. Colaneri, "Railway collaborative ecodrive via dissension based switching nonlinear model predictive control," *European Journal of Control*, vol. 50, pp. 153–160, 2019.

[25] A. Bemporad and M. Morari, "Control of systems integrating logic, dynamics, and constraints," *Automatica*, vol. 35, no. 3, pp. 407–427, 1999.

[26] R. Gondhalekar and J. Imura, "Recursive feasibility guarantees in move-blocking MPC," in *IEEE 46th Conference on Decision and Control*, New Orleans, LA, USA, Dec. 2007, pp. 1374–1379.
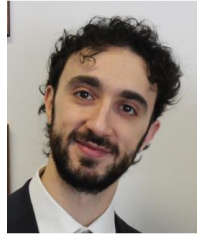
Gian Paolo Incremona (M'10, S'23) is Associate Professor of Automatic Control at Politecnico di Milano. He was a student of the Almo Collegio Borromeo of Pavia, and of the Institute for Advanced Studies IUSS of Pavia. He received the Bachelor and Master Degrees summa cum laude in Electric Engineering, and the Ph.D. Degree in Electronics, Electric and Computer Engineering from the University of Pavia in 2010, 2012 and 2016, respectively. From October to December 2014, he was with the Dynamics and Control Group at the Eindhoven Technology University, The Netherlands. He was a recipient of the 2018 Best Young Author Paper Award from the Italian Chapter of the IEEE Control Systems Society, and since 2018 he has been a member of the conference editorial boards of the IEEE Control System Society and of the European Control Association. At present, he is Associate Editor of the journal Nonlinear Analysis: Hybrid Systems and of International Journal of Control. His research is focused on sliding mode control, model predictive control and switched systems with application mainly to robotics, train control and power plants.

Alessio La Bella received the B.Sc. and M.Sc. in Automation Engineering cum laude from Politecnico di Milano in 2013 and 2015, respectively. In 2016, he received the Alta Scuola Politecnica Diploma, together with the M.Sc. in Mechatronics Engineering cum laude at Politecnico di Torino. He received the Ph.D. Degree cum laude in Information Technology at Politecnico di Milano in 2020. In 2018, he was visiting researcher at the Automatic Control Lab of the École Polytechnique Fédérale de Lausanne, Switzerland. From 2020 to 2022, he worked as Research Engineer at Ricerca sul Sistema Energetico - RSE SpA, designing and implementing advanced predictive control systems for district heating networks and large-scale battery plants, in collaboration with industrial companies and energy utilities. In 2022, he joined Politecnico di Milano as Assistant Professor at Dipartimento di Elettronica, Informazione e Bioingegneria. His research interests concern the theory and design of predictive, multi-agent and learning-based control systems, with particular emphasis on practical challenges arising from the upcoming energy transition. He was recipient of the Dimitris N. Chorafas Prize in 2020.

Patrizio Colaneri received the Laurea degree in electrical engineering from the Politecnico di Milano, Milan, Italy, in 1981, the Ph.D. degree in Automatic Control from the Italian Ministry of Education and Research, Italy, in 1988. He is a Full Professor of Automatic Control at Politecnico di Milano, Italy, where he served as the Head of the Ph.D. School on ICT (2007–2009). He held visiting positions with the University of Maryland, Hamilton Institute of the National University of Ireland, and at the Institute for Design and Control of Mechatronic Systems, Johannes Kepler University in Linz, Austria. He served IFAC and IEEE CSS in many capacities in journals and conferences. In particular, he was Associate Editor of Automatica for six years (certificate of outstanding service), a Senior Editor of IEEE TAC for eight years, the IPC Chair of the IFAC Symposium ROCOND in Milan in 2003, the IPC Vice Chair of the CDC in Florence in 2013, the IPC Chair of the IEEE Multi Conference on System and Control in Buenos Aires in 2016. He has been a Senior Editor of the IFAC journal Nonlinear Analysis: Hybrid Systems for six years. His main research interests are in the area of periodic systems and control, robust filtering and control, switching control, and railway automation. He authored/coauthored about 270 papers and seven books (three in Italian). Dr. Colaneri was a member of the IFAC Technical Board and is currently the Chair of the Italian National Member organization. He is a Fellow of IFAC and IEEE and received the certicate of outstanding service of IFAC.